

Check for updates

Original Manuscript



# Effect of nanoscale interface modification on residual stress evolution during composite processing

Journal of Composite Materials 2023, Vol. 0(0) 1–17 © The Author(s) 2023 Article reuse guidelines: sagepub.com/journals-permissions DOI: 10.1177/00219983231179522 journals.sagepub.com/home/jcm



### Deepak Kumar, Marie Claire Dusabimana, Marwan Al-Haik<sup>2</sup> and Sirish Namilae

#### **Abstract**

The interface characteristics of the matrix and fibers significantly influence the evolution of residual stress in composite materials. In this study, we provide a methodology for reducing the residual stress in laminated composites by modifying the thermomechanical properties at the fiber—matrix interface. A hydrothermal chemical growth method was used to grow Zinc Oxide nanowires on the carbon fibers. We then utilized a novel digital image correlation approach to evaluate strains and residual stresses, in situ, throughout the autoclave curing of composites. We find that interface modification results in the reduction of residual stress and an increase in laminate strength and stiffness. Upon growing ZnO NWs on the carbon fibers, the maximum in situ in-plane strain components were reduced by approximately 55% and 31%, respectively, while the corresponding maximum residual stresses were decreased by 50.8% and 49.33% for the cross-play laminate [0°/90°] layup in the x and y directions, respectively. For the [45°/-45°] angle ply layup in the x-direction, the strain was decreased by 27.3%, and the maximum residual stress was reduced by 41.5%, whereas in the y-direction, the strain was decreased by 166.3%, and the maximum residual stress was reduced by 17.8%. Furthermore, mechanical testing revealed that the tensile strength for the [45°/-45°] and [0°/90°] laminates increased by 130% and 20%, respectively, with the interface modification.

#### **Keywords**

Carbon fiber, composites, nanowires, interface, surface modification, residual strain, residual stress

#### Introduction

Carbon fiber-reinforced polymer composites (CFRPs) are among the most widely used structural materials in the aerospace industry because of their high strength-to-weight ratio, better corrosion resistance, and improved fatigue life compared with commonly used metals. However, CFRPs have some drawbacks, such as low impact resistance and interlaminar delamination. The interfaces between the fiber and matrix play a crucial role in load transfer from the weak matrix to the strong fibers. This has led to the emergence of different methods of interface modification to produce better CFRPs that are strong, light, and delamination resistant. Furthermore, interface modification can also enable multifunctional capabilities.

One method for interfacial modification is reinforcing the interface region by growing nanoscale species on the fiber. Nano-species with different morphologies, such as nanorods, nanowires, nanotubes, including carbon nanotubes (CNTs), metal—organic frameworks (MOFs), and ZnO nanowires (NWs), have been used for this purpose. For instance, growing CNTs on carbon fibers can enhance their

mechanical properties, including their ductility and tensile strength. After growing CNTs on carbon fibers, the ductility and on- and off-axis tensile strength increased by 35%, 11%, and 16%, respectively.<sup>4</sup> Likewise, MOF-modified fibers' flexural and tensile strengths increased to approximately 81.3% and 177.9%, respectively.<sup>5</sup> In addition, MOFs can reduce the wear of composites by 44.4% and increase the friction coefficient compared with regular composites.<sup>5</sup> Similarly, by growing ZnO NWs on carbon fibers, both the damping and flexural rigidity of composites can be enhanced.<sup>6</sup>

#### Corresponding author:

Sirish Namilae, Department of Aerospace Engineering, Embry-Riddle Aeronautical University, I Aerospace Blvd, Daytona Beach 32114-3900, FL, USA.

Email: namilaes@erau.edu

<sup>&</sup>lt;sup>1</sup>Department of Aerospace Engineering, Embry-Riddle Aeronautical University, Daytona Beach, FL, USA

<sup>&</sup>lt;sup>2</sup>Department of Mechanical Engineering, Kennesaw State University, Marietta, GA, USA

In addition to improving the mechanical properties, fiber modification has the potential to impart multifunctionality to composites. For example, carbon fibers modified with CNTs exhibited increased optical absorption from visible to infrared light. This makes the carbon fiber/CNTs hybrids an excellent fit for photothermal conversion applications. Composites with carbon fibers modified by ZnO NWs can potentially be used for energy-harvesting applications owing to the piezoelectric and semiconducting behaviors of ZnO nanowires. Other applications for ZnO nanowiresmodified fibers include structural health monitoring for damage detection and sensing/actuating applications.

Because of the aforementioned structural and multifunctional advantages, we used ZnO NWs for the interface modification in this study. One approach to growing ZnO NWs on carbon fibers is metal-organic chemical vapor deposition (MOCVD). By applying this method to grow ZnO nanowires, the adhesion energy could be significantly increased. Owing to the strong bonding between the nanorods, carbon fiber, and epoxy molecules, the mechanical properties of the hybrid composite were improved because of the increased surface area. 10 Comparably, using atomic layer deposition (ALD) and the hydrothermal method, it was found that the interlaminar shear strength (ILSS) could be improved by 99% when using ZnOmodified carbon fibers. 11 A smaller diameter of the ZnO nanorods was also found to result in higher interfacial shear strength. 12 Compared with MOCVD and ALD, the hydrothermal chemical growth method is a low-temperature method: therefore, it does not introduce fiber degradation and can be carried out NWs without specialized tooling. Moreover, the hydrothermal chemical growth method is scalable to large structures. Because of these advantages, we utilized this approach for the ZnO NWs growth.

Composite materials often have residual stress at different scales. Macroscale residual stresses can arise between different structural components due to external constraints, e.g., dimensional mismatch during assembly. 13 Mesoscale residual stress developed between different plies of a composite laminate due to differences in the response of individual plies with different orientations, subject to the same thermomechanical loading and constraints. 14 At the microscale, the mismatch of the thermal characteristics of the resin and fiber are the root causes of residual stress buildup. The coefficients of thermal expansion (CTE) of the resin and the fiber differ substantially. Tensile residual stresses develop in the matrix, and compressive stresses develop in the fiber because of the resins' higher thermal expansion coefficient than the fibers. 15 The residual stress highly affects the overall performance of composite materials, including reducing their strength, <sup>16</sup> decreasing the apparent Young's modulus, 17 premature failure, warping, dimensional instability, 18 fiber waviness, and cracking. Interface modification techniques can reduce residual stress by reducing the dissimilarities between the fiber and matrix properties. Adding carbon nanofibers to the matrix efficiently reduces the residual stress in laminated composites because the nanofiller increases the stiffness of the matrix, lowers its coefficient of thermal expansion (CTE), and brings it closer to the fiber properties. Nishino et al, 2 used tungsten zirconium phosphate (ZWP) particles to reduce the residual stress of polyetheretherketone (PEEK). A 62% reduction in the CTE was achieved with 40 vol% ZWP. While the above studies focused primarily on modifying the matrix to reduce residual stresses, to the best of our knowledge, no published studies have attempted to minimize residual stresses by modifying fibers. Additionally, no studies have documented the in situ evolution of residual stresses with enhanced interfaces.

A technique for characterizing processing-induced defects during the production of composite laminates using digital image correlation (DIC) was developed by our team members.<sup>23</sup> The in situ method was adapted to continuously evaluate the residual stress during the curing process of composite laminates.<sup>24</sup> Different laminate layup arrangements, both symmetric and asymmetric, were used to describe residual stress development during the composite processing. In addition, methods for reducing residual stresses using a cure cycle design have been discussed.<sup>25</sup> Here, we extend this approach to investigate the effect of interface modification on residual stress evolution.

We hypothesize that nanoscale modification of the fibermatrix interface results in the improvements in the mechanical properties and reduces the residual stresses at larger length scales. We achieve the nanoscale interface enhancement by growing ZnO nanowires on carbon fibers using a hydrothermal chemical growth technique. This is a low temperature technique, therefore does not degrade the carbon fibers. An in situ experimental method was used to observe the effect of interface modification on the evolution of residual stresses developed during curing. This approach utilizes digital image correlation (DIC) of the composite panels during curing, through a specially designed autoclave with viewports. Several microstructural and thermomechanical characterization techniques have been utilized to analyze the enhanced hybrid composites. While several studies utilized matrix modification to reduce residual stresses, this study is focused on fiber and interface modification. The subsequent section details the experimental and analytical methods and is followed by results and discussion.

#### **Methods**

#### Materials

The list of materials used in this research includes Thornell T650/35 plain-woven PAN-based structural carbon fibers

procured (Solvay Inc); Aeropoxy PR 2032 resin and PH 3660 hardener (PTM&W Inc.); Nitric acid (ACS reagent, 70%) from Sigma-Aldrich; Zinc acetate dihydrate (ACS, 98.0%—101.0%, crystalline) from Alfa Aesar; Sodium hydroxide (flake, 98%) from Alfa Aesar; Ethyl alcohol (pure, ACS reagent, ≥99.5%) from Sigma-Aldrich). Zinc Nitrate hexahydrate (99%, metals basis, crystalline) from Alfa Aesar; Hexamethylenetetramine (HMTA) (ACS, 99+%, Solid) from Alfa Aesar.

#### Fiber modification with ZnO nanowires

The carbon fibers were de-sized inside a tube furnace (OTF-1200X from the MTI Corporation) at 550°C for 30 min under an inert environment. The growth of ZnO NWs on carbon fibers involves three main processes: activation, seeding, and growth, as shown in Figure 1. After de-sizing, the carbon fiber fabric was cut into 12.5 cm × 12.5 cm pieces. The activation process was achieved by soaking the fiber fabric in a diluted nitric acid solution for 24 h and then rinsing the fiber with DI water repeatedly to achieve a pH of 7.0. The seeding solution was prepared by stirring a solution of 100 mg zinc acetate dihydrate, 40 mg sodium hydroxide, and 400 mL ethyl alcohol at 400 r/min for 1 h. Each activated fiber fabric was then dipped in the solution for 2 min and dried in an oven for 15 min at 150°C; this process was repeated five times to ensure good coverage of ZnO seeds. The growth solution was prepared by mixing a 13.98 g zinc nitrate hexahydrate and 1,800 mL DI water using an ultrasonic processor for 40 min. Separately, 6.3 g of HMTA and 1,800 mL DI water solution were mixed using the sonicator for 40 min. The two solutions were remixed and agitated using a tip-sonicator for 40 min. Subsequently, the growth process was performed by soaking each piece of the seeded fibers in 600 mL of the growth solution for 6 h at 90°C inside an oven. The growth container is covered with an aluminum foil to reduce evaporation. The fibers were then dried in an oven at 150°C for 48 h. The protocol for the ZnO nanowires was developed by our team in a previous study.<sup>26</sup>

#### Composite samples preparation

Two-ply composite laminates with  $[0^{\circ}/90^{\circ}]$  and  $[45^{\circ}/-45^{\circ}]$  configurations were prepared using the hand layup process. The composites contained 60% fibers, and 40% epoxy matrix

by weight. The matrix is prepared by mixing Aeropoxy PH2032 resin and PR3032 hardener in a 100:27 weight ratio. The laminates were cured in an ACS Process Systems autoclave (EC2X4-200P800F-2S2P4T). The curing process lasted for 150 min at 93°C before cooling to room temperature in a controlled autoclave. These samples were used for thermomechanical and microstructural characterizations described in Section *Microstructure, mechanical, and thermomechanical characterization*. The in situ process characterization during curing is discussed separately in Section *In-situ process characterization*.

#### In-situ process characterization

Another set of two-ply composite laminates with [0°/90°] and [45°/-45°] configurations were prepared using the same wet layup process. A high-contrast speckle pattern is required for in situ DIC applications. This cannot be achieved at the beginning of curing because of the wet upper surface. The wet layup sample was initially cured in an oven at a rate of 5°C/min to reach 93°C and held for 12-14 min. The sample was cured by about 15%–20% in this step. Highcontrast random speckle patterns were sprayed on the partially cured laminate surface using white hightemperature spray paint. The samples were then transferred to the autoclave. The autoclave was preheated to 93°C. The samples were cured under a Nitrogen pressure of 24.13 bar for an additional 150 min before cooling to room temperature in a controlled autoclave environment. As illustrated in Figure 2, the autoclave employed in this study was specially designed with two borosilicate glass viewports, an interior light viewport, and a J-type thermocouple to detect the internal temperature. A 3D digital image correlation (DIC) was set up by pointing through the custom glass viewport of the autoclave. This DIC setup was used to capture images of the composite samples at intervals of 5 s throughout the curing process. The movement of the speckled pattern caused by ply deformation during the curing process was analyzed using VIC-3D software.

## Microstructure, mechanical, and thermomechanical characterization

Microstructure characterization. After growing ZnO NWs on the carbon fibers, a strand of fibers was imaged to study the



Figure 1. ZnO nanowires growth process.

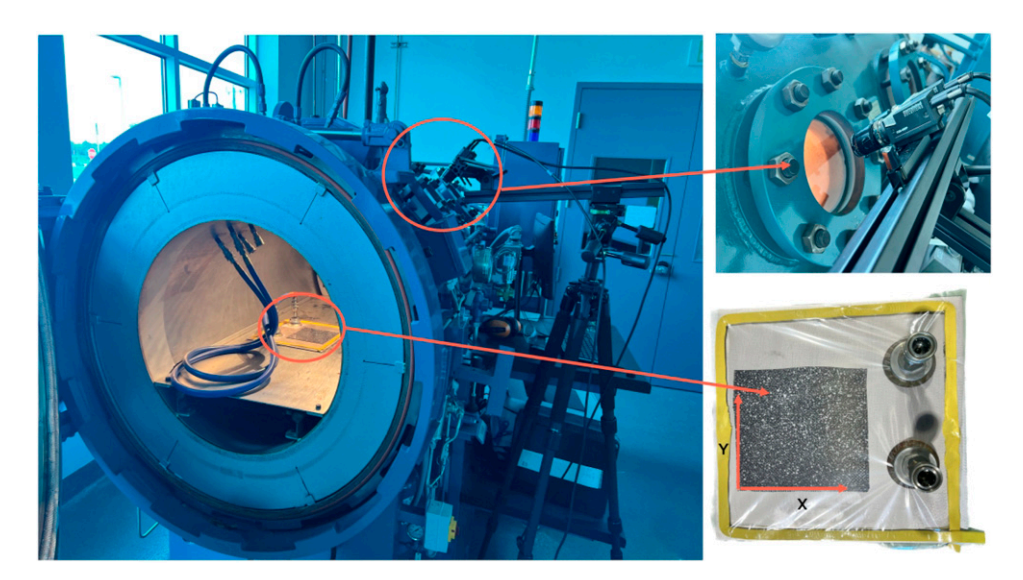


Figure 2. Autoclave with glass viewports. Insets show the DIC setup and schematic of the sample location.

ZnO NWs growth. The fibers were sputter-coated with gold before imaging. Then, using an FEI Quanta 650 scanning electron microscope (SEM), the micrographs shown in Figure 3 were produced. Images were used to examine the topology and density of the grown ZnO nanowires.

Tensile test. To the possible extent, the tensile tests were performed according to ASTM D3039/D3039M-17 standards.  $^{27}$  G-10 tabs were placed on two opposite ends of the tensile specimen to enable adequate gripping. The applied load was measured using a 10 kN load cell of the MTS criterion model 43, and the strain was measured using a 3D digital image correlation DIC (Correlated Solutions, Inc.). Five specimens,  $125 \times 12.7 \times 0.65$  mm each, with the modified and unmodified fibers for each configuration, were tested in tension at a rate of 3 mm/min (0.05 m/s). This rate, different from that suggested in the ASTM standard, was chosen to better correlate the testing frame data acquisition and the DIC imaging rate, which operate at 1.0 Hz frequency. Stress versus strain curves are shown in Figure 4.

Dynamic mechanical analysis (DMA). A dynamic mechanical analyzer (DMA 800, PerkinElmer) was used to estimate the damping parameter (tan  $\delta$ ) and the storage modulus of the samples. A three-point bending fixture was used to load samples. A temperature sweep between 30 and 90°C at a frequency of 1.0 Hz was performed on each sample. Each sample was approximately 44.5 mm  $\times$  6.4 mm  $\times$  1.6 mm, following the measurement limits recommended in the ASTM D7028-07 standards. The DMA results are shown in Figure 5.

2Differential scanning Calorimetry (DSC). Mettler Toledo's differential scanning calorimeter was used to analyze the

energetics and cure kinetics of the Aeropoxy resin. Approximately 13–18 mg of the resin and hardener mixture in the same ratio used for the composite processing (100:27) was added to the crucibles. A constant nitrogen flow rate of 20 mL/min was used. The resin was heated at three different rates 8°C/min, 12°C/min, and 16°C/min from -25°C to 250°C. All tests were conducted using an empty crucible as a reference. The area under the peak of the exotherm is used to estimate the total heat flow ( $\Delta$ H). The curing rate of the resin ( $\alpha$ ) was estimated using the measured heat flow ( $\phi$ ) and enthalpy of the curing reaction, as shown in equation (1).<sup>29</sup>

$$\frac{d\alpha}{dt} = \frac{\emptyset}{\Delta H} \tag{1}$$

The DSC experiments were carried out at three different heating rates to observe the effect of the increased heating rate on the curing behavior of the resin. The kinetics of resin polymerization is further calculated using equation (2).<sup>30</sup> The logarithmic form of equation (2) can be used to calculate the activation energy for the curing process.

$$\frac{da}{dt} = Ae^{-\left(\frac{E_d}{N\theta}\right)} \tag{2}$$

Where  $E_a$  is the activation energy, R is the universal gas constant, and  $\theta$  is the temperature.

Residual stress calculation. The liberated strain approach was used to calculate the residual stress based on the surface strain measured using DIC as shown in equation (3). The residual strain,  $\varepsilon_R$ , is calculated as the difference between the total measured strain  $\{\varepsilon\}$  and the strain associated with

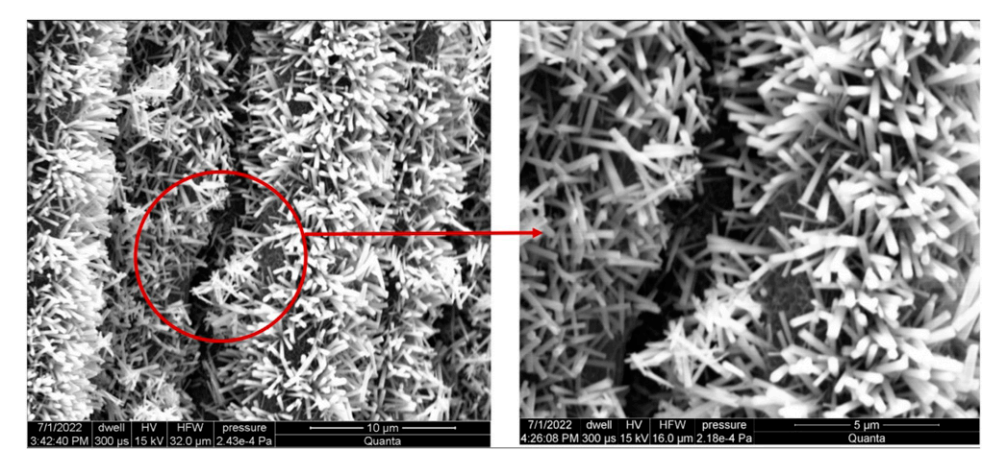


Figure 3. SEM micrographs, at different magnifications, of the ZnO nanowires growth on the carbon fiber surface.

thermal expansion  $\alpha$   $\Delta\theta$ . Here,  $\alpha$  is the coefficient of thermal expansion and  $\Delta\theta$  is the temperature gradient. The transformation matrix  $\{T\}$  was used to transform the strain components from the local to global axes. This approach was discussed in detail in a previous study.<sup>24</sup>

$$E_R = \{T\}\{\varepsilon\} - \alpha \Delta \theta \tag{3}$$

The approximate value of the overall CTE in both the xand y-directions was calculated using the standard micromechanics formulation provided in equation 4.

$$\begin{bmatrix} \alpha_{x} \\ \alpha_{y} \\ \alpha_{z} \end{bmatrix} = \{T\}^{t} \begin{bmatrix} \alpha_{1} \frac{E_{F} \alpha_{F} V_{F} + E_{m} \alpha_{m} V_{m}}{E_{F} V_{F} + E_{m} V_{m}} \\ \alpha_{2} = (1 + V_{F}) \alpha_{F} V_{F} + (1 + V_{m}) \alpha_{m} V_{m} = \alpha_{1} \left(V_{F}^{2} + V_{m}^{2}\right) \end{bmatrix}$$

The subscripts F and m denote the fiber and matrix, respectively.<sup>31</sup> E is the Young's modulus, and V is the volume fraction of the phase. The composite is cured at 93°C, therefore,  $\alpha \Delta \theta$  of 63°C with a range from 30°C to 93°C is considered. By using the manufacturer-provided properties of the T650 fiber  $\alpha_F = 0.60 \times 10^{-6}$ ,  $E_F = 255 \times 10^{-6}$  $10^9$  Pa, and the Aeropoxy matrix  $\alpha_m = 3.7 \times 10^{-5}$ ,  $E_m =$  $3.12 \times 10^8$  Pa, the coefficient of thermal expansion,  $\alpha_1$ , was found to be approximately  $6.66 \times 10^{-7}$  oC where  $\alpha_2$ , was found to be approximately  $3.55 \times 10^{-5}$  C. Due to its growth pattern, the ZnO NWs growth was not expected to alter the fibers' longitudinal expansion coefficient change. However, it could alter the thermal expansion of the matrix at the interface region; the volume of the interface region is much smaller than that of the matrix. Therefore, the same thermal expansion coefficient was used for the laminae with and without ZnO modification.

After the residual strain calculation, the DMA experimental data, shown in Figure 5, were used to calculate

the temperature-dependent modulus for both composite layups. This was then used to calculate the stiffness matrix Q. Finally; the residual stress was calculated using equation 5.

$$\{\sigma_R\} = \{Q(\theta)\} \{\varepsilon_R\}$$
 (5)

Where Q is the temperature-dependent 2D orthotropic reduced stiffness matrix. This process was repeated for the residual stress calculations for all the samples presented in this study.

#### Results and discussion

#### Microstructural characterization

The micrographs in Figure 3 show that the ZnO NWs were successfully grown on the fibers. The hydrothermal chemical growth method yielded a uniform coverage of radially-grown ZnO NWs of uniform lengths and diameters. The nanowires grew radially on the fibers' surface with almost identical morphology. The length of the nanowires is around 2.0  $\mu$ m and the diameter is around 100 nm.

#### Mechanical characterization

Tensile test results. All the results presented in this study are based on at least three sets of experiments for each case. In Figures 4, 5, 9–14, the results for reference composite laminate are shown by dashed lines, and for ZnO-modified composite laminate solid line is used. Each curve corresponds to one experiment.

Figure 4 shows stress-strain plots for the composites made with fibers without ZnO and those made with ZnO nanowires. For the [0°/90°] configuration, the strength increased by 20% from a maximum value of approximately 500 MPa–600 MPa due to the fiber modification. For the [45°/-45°] laminate, the percentage increase in strength was

more significant. It increased by about 130%, from 35 MPa to 80 MPa.

Using the linear portion of the graphs shown in Figure 4, the apparent elastic modulus for the [0°/90°] composite laminate improved by 9% from 42.97 GPa for the reference composite to 46.81 GPa for the hybrid composite. The improvement for the [45°/-45°] laminate was more noticeable, and the modulus increased by 280% from 3.88 GPa to 14.70 GPa for the hybrid composite. Similar observations on the improvement in the apparent elastic modulus due to the addition of ZnO NWs have been reported in previous studies. <sup>32</sup>

There was a significant increase in the off-axis values upon fiber modification for both strength and stiffness. This suggests that ZnO NWs growth may have improved the matrix performance at the interface because the off-axis properties are generally dominated by matrix behavior.<sup>33</sup>

Dynamic mechanical analysis results. DMA testing was used to determine the temperature dependence of the elastic behavior. We approximated the composite's room-temperature apparent elastic modulus to be the same as the room-temperature storage modulus. Because of the low-frequency conditions, we assumed that the temperature variation of the apparent elastic modulus is equivalent to the temperature variation of the storage modulus. Therefore, the temperature-dependent apparent elastic modulus for the composites was estimated from the results of the DMA

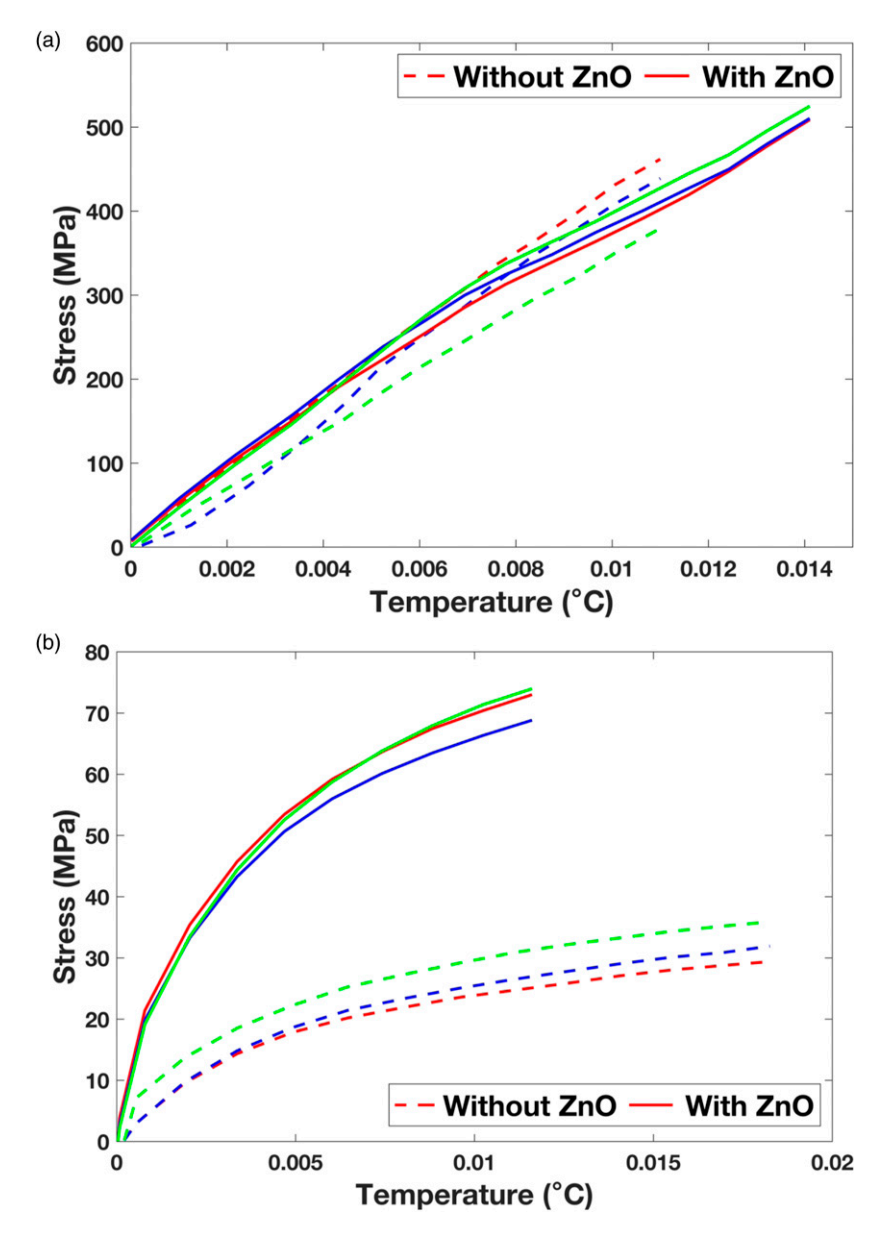


Figure 4. Tensile test results for the hybrid and reference composites for (a) [0°/90°], and (b) [45°/-45°] laminates.

experiment using the temperature-dependent storage modulus. The room temperature apparent elastic modulus was obtained from the tensile test. For all composite samples. The apparent elastic modulus variation with temperature was calculated by multiplying the storage modulus variation with temperature by the ratio of room temperature apparent elastic modulus (from the tensile test) to the average storage modules (from the DMA test) at room temperature.

Composites comprising ZnO-modified fibers exhibited higher apparent elastic moduli than the reference composites. The elastic properties generally decreased at higher temperatures mainly due to matrix degradation. Additionally, for the  $[0^{\circ}/90^{\circ}]$  composites, this rate of decrement/

increment was consistent for the reference and the ZnO-modified laminates, as shown in Figure 5(a). For the [45°/-45°] composite laminate, the rate of degradation in the elastic properties was higher for the ZnO-modified fiber composite than for the reference composite, as shown in Figure 5(b). The effective mechanical properties of the [45°/-45°] configuration are more matrix-dependent than the [0°/90°] configuration. Therefore, the elastic properties are expected to be relatively poor at high temperatures. Because of the ZnO NWs growth, the modified composite has a much higher room temperature apparent elastic modulus for the [45°/-45°] orientation. Therefore, it starts from a higher value and decreases at a higher rate compared to the reference sample.

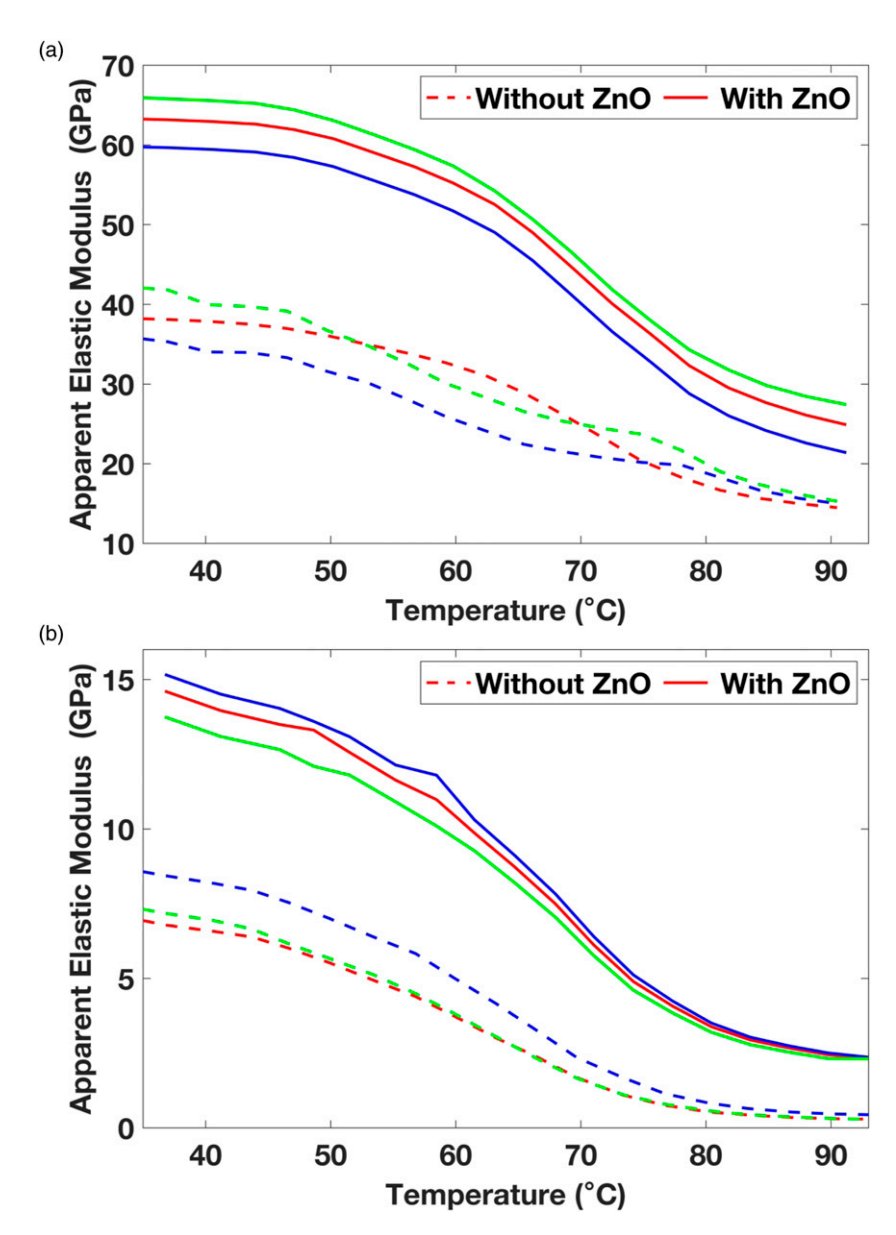
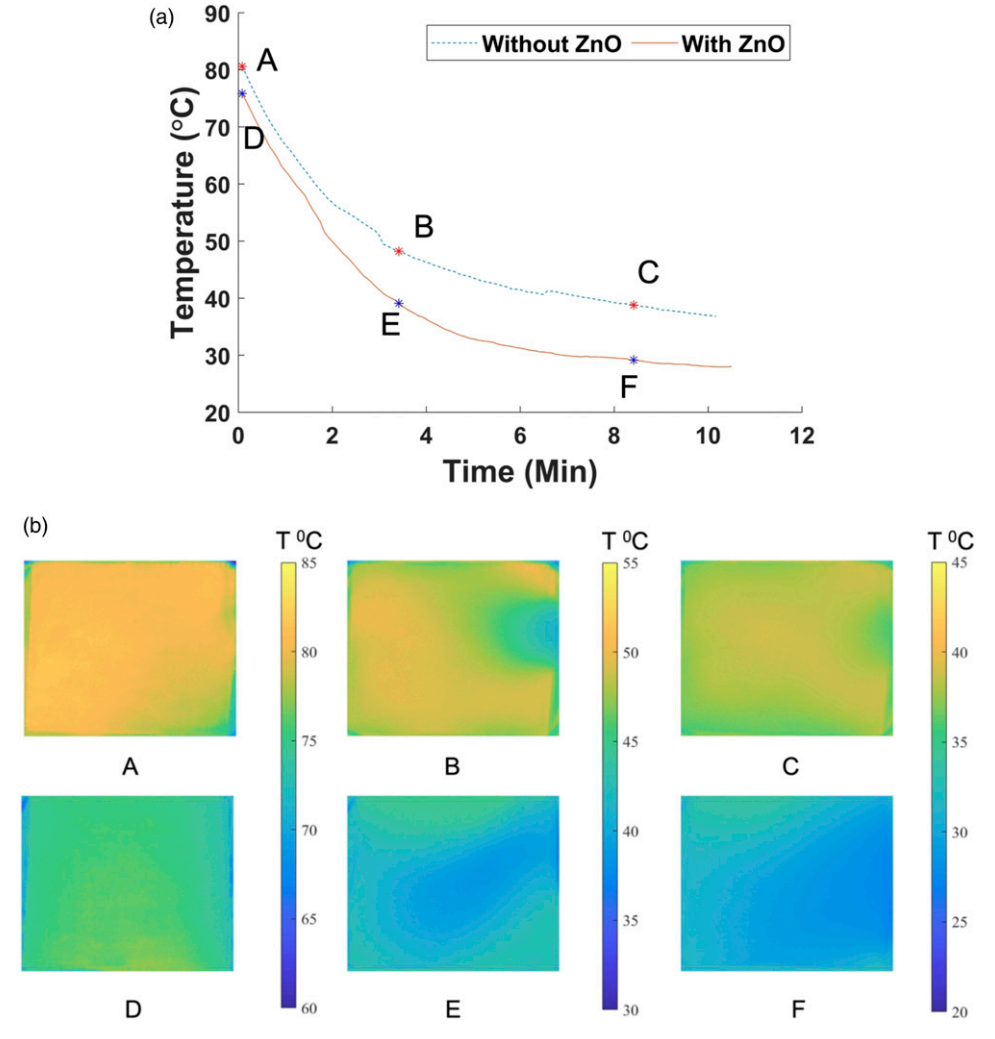


Figure 5. Temperature variation of apparent elastic modulus for (a) [0°/90°], and (b) [45°/-45°] laminates.

#### Thermal imaging and cure kinetics

After processing the composites in the autoclave, a thermal camera was used to monitor the cooling profiles of the composites. The cooling rate of the composites with ZnOmodified fibers was higher than that of the reference composite, as shown in Figure 6(a). The exposed surface area of a single fiber is significantly increased by the ZnO NWs, as seen in the SEM images in Figure 3, leading to a higher heat transfer rate than the reference configuration. The temperature profile shown in Figure 6(a) was divided into two segments for cooling rate comparison. For the composites made with reference fibers, the cooling rate in sections A-B was 8.50°C/min, and in sections B-C was 2.55°C/min. Whereas, for the composites made with ZnOenhanced fibers, the cooling rate for sections D-E is 10.57°C/min and 1.70°C/min for sections E-F, respectively. By comparison, the ZnO nanowire's growth increased the cooling rate by 2.07°C/min. ZnO growth on the fiber acts as a nanoscale cooling fin, which increases the heat transfer between the fiber and the matrix. Figure 6(b) shows the thermal images of different cooling segments for reference and ZnO-modified composite.

At a heating rate of  $16^{\circ}$ C/min, the maximum degree of cure was achieved at approximately  $150^{\circ}$ C, whereas this value was smaller at lower heating rates. In this case, the temperature-independent activation energy for curing ( $E_{\alpha}$ ) is 104.9 KJ/mol. The thermal imaging and DSC show that the curing process for ZnO NWs-modified composite happens at a faster rate, especially in the interface region, compared to the reference composite. This has implications for residual stress evolution, as shown in subsequent sections. The peak of the heat flow shifted to a higher temperature value, and the maximum value of the heat flow also increased as the heating rate increased from  $8^{\circ}$ C/min to  $16^{\circ}$ C/min, as shown in Figure 7(a). The variation in the



**Figure 6.** (a) Cooling history of reference and ZnO modified composite for the  $[0^{\circ}/90^{\circ}]$  laminate. (b) Thermal profile of reference and ZnO modified composite for the  $[0^{\circ}/90^{\circ}]$  laminate.

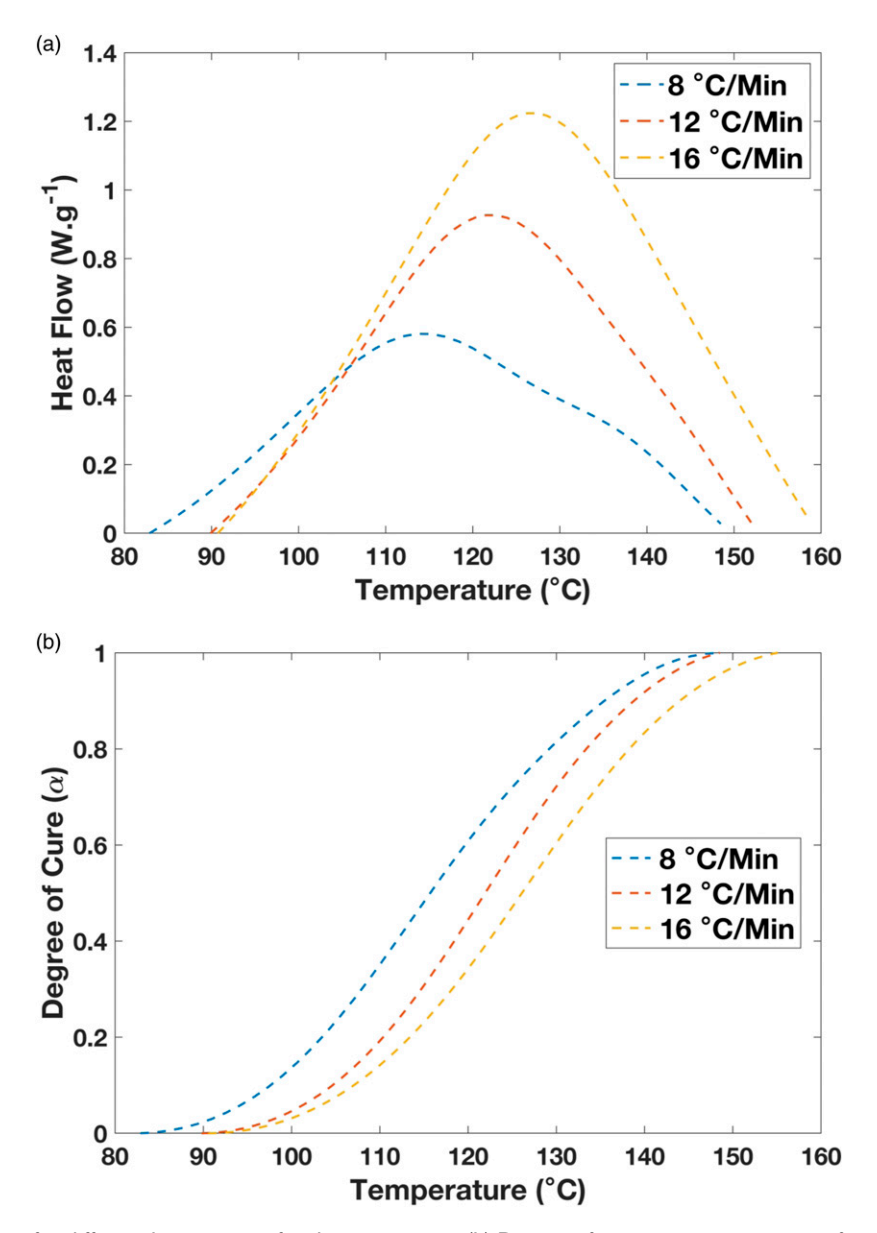


Figure 7. (a) Heat flow for different heating rates for the epoxy resin. (b) Degree of cure versus temperature for different heating rates.

degree of cure with temperature for different heating rates is shown in Figure 7(b).

#### Processing strain - DIC results

The surface strain was measured by considering the vacuum direction to be X and the direction perpendicular to the vacuum to be Y, as shown in Figure 2. The initial increase in strain during the heating phase was primarily due to the thermal expansion of the fibers and matrix. When the isothermal stage is achieved, the development of strain is influenced by both cure shrinkage and thermal effects. DIC surface strain measurement during curing is shown in Figure 8.

As seen in Figure 9, composites made using the reference fibers exhibit higher  $\varepsilon_x$  and  $\varepsilon_y$  values than composites with modified fibers. The highest recorded value of  $\varepsilon_x$  for the  $[0^{\circ}/90^{\circ}]$  reference laminate was  $1.789 \times 10^{-3}$ , which was noticed at approximately 50 min through the curing process, as shown in Figure 9(a). After approximately 55 min of curing, the maximum  $\varepsilon_y$  strain of  $11.8 \times 10^{-4}$  was observed, as shown in Figure 9(b). On the other hand, a maximum  $\varepsilon_x$  of  $0.792 \times 10^{-3}$  was noticed in the  $[0^{\circ}/90^{\circ}]$  laminate made with the ZnO-modified fibers approximately 20 min into the curing process, as shown in Figure 9(a). After approximately 38 min of curing, a maximum  $\varepsilon_y$  value of  $8.12 \times 10^{-4}$  was noticed, as shown in Figure 9(b).

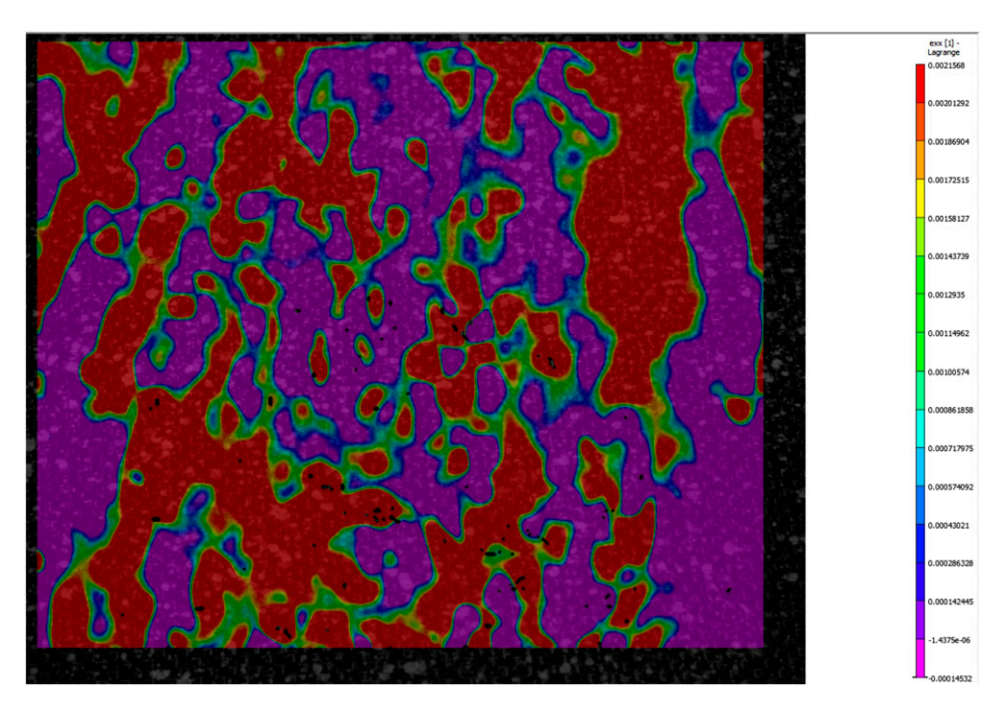


**Figure 8.** Measured surface strain  $\varepsilon_{x}$  for reference sample by DIC

Therefore, by incorporating ZnO NWs in the [0°/90°] composite laminate, the maximum  $\varepsilon_x$  and  $\varepsilon_y$  were reduced by 55% and 31%, respectively. As a result of ZnO NWs growth, the isothermal stage average  $\epsilon_{\boldsymbol{x}}$  decreased by 61.15% from  $1.91 \times 10^{-3}$  to  $7.42 \times 10^{-4}$ , while the isothermal stage average  $\epsilon_y$  decreased by 43.9% from 1.155  $\times$  $10^{-3}$  to  $6.48 \times 10^{-4}$ . The strain  $\varepsilon_y$  is lower for both composite laminates because  $\varepsilon_x$  is measured along the vacuum line direction. The coefficients of thermal expansion for epoxy and fiber are  $3.7 \times 10^{-5}$  and  $0.60 \times 10^{-6}$ , respectively; therefore, in the cooling phase, the volumetric shrinkage of the matrix is expected to be higher than the fiber shrinkage. This explains the formation of compressive residual strain in the fibers and matrix. The transfer of these strains and stresses is governed by the interface bonding and load-sharing properties of the fiber and matrix.<sup>34</sup> Because of the higher cooling rate, higher load sharing, and stronger interface bonding, the volumetric shrinkage is higher in ZnO-enhanced composite laminates, which results in more compressive strain compared to reference composite laminates.

Similar behavior was observed for the [45°/-45°] angle-ply laminate. For the composites made using the reference fibers, a maximum  $\epsilon_x$  of  $1.05\times 10^{-3}$  was observed after approximately 20 min of curing. For the composites with ZnO modification, a maximum  $\epsilon_x$  of  $0.76\times 10^{-3}$  was observed after approximately 40 min of curing. Due to ZnO modification, a 27.61% reduction in the maximum value of  $\epsilon_x$  is observed. While the isothermal stage average  $\epsilon_x$  decreased by 28.30% from 8.66  $\times$   $10^{-4}$  to 6.21  $\times$   $10^{-4}$ , as shown in Figure 10(a).

For  $\varepsilon_{v}$ , the [45°/-45°] composite laminate exhibited similar behavior. As shown in Figure 10(b), the  $\varepsilon_v$  for the composites made using fibers without ZnO is tensile, with a maximum value of  $1.63 \times 10^{-3}$  after approximately 130 min of curing. The  $\varepsilon_v$  for the composites made using fibers with ZnO is compressive, with a maximum value of  $-1.08 \times 10^{-3}$  observed approximately after 125 min of curing, resulting in a reduction of 166.26% in  $\epsilon_{y}$ . While the isothermal stage average  $\varepsilon_{\rm v}$  decreased by 141.11% from 1.34 × 10<sup>-3</sup> to -5.51 × 10<sup>-4</sup>, as shown in Figure 10(b). In general, the measured strains in the angle-ply [45°/-45°] laminate were smaller than those for the cross-ply  $[0^{\circ}/90^{\circ}]$ . This is due to the balanced nature of the angle-ply where the normal-shear reduced stiffness elements and the thermal shear expansion in the 45° ply are equal in magnitude but opposite in sign to the values in the  $-45^{\circ}$  ply eliminating both the thermal shear force and thermal shear moment. While in the cross-ply laminate, only the thermal shear force vanishes, but the thermal moment does not, which leads to higher thermal strains and residual stresses.

#### Residual stress evolution

For the  $[0^{\circ}/90^{\circ}]$  laminate, the residual stress was plotted with respect to curing time, as shown in Figure 11 and Figure 12. Up until 100 min of curing, a gradual increase in residual stress was observed. For composites constructed using reference fibers, the residual stresses rapidly increased from 100 min to 150 min of curing, reaching a maximum value of -59 MPa in the *x*-direction and -225 MPa in the *y*-direction, as shown in Figure 11. A similar trend in the

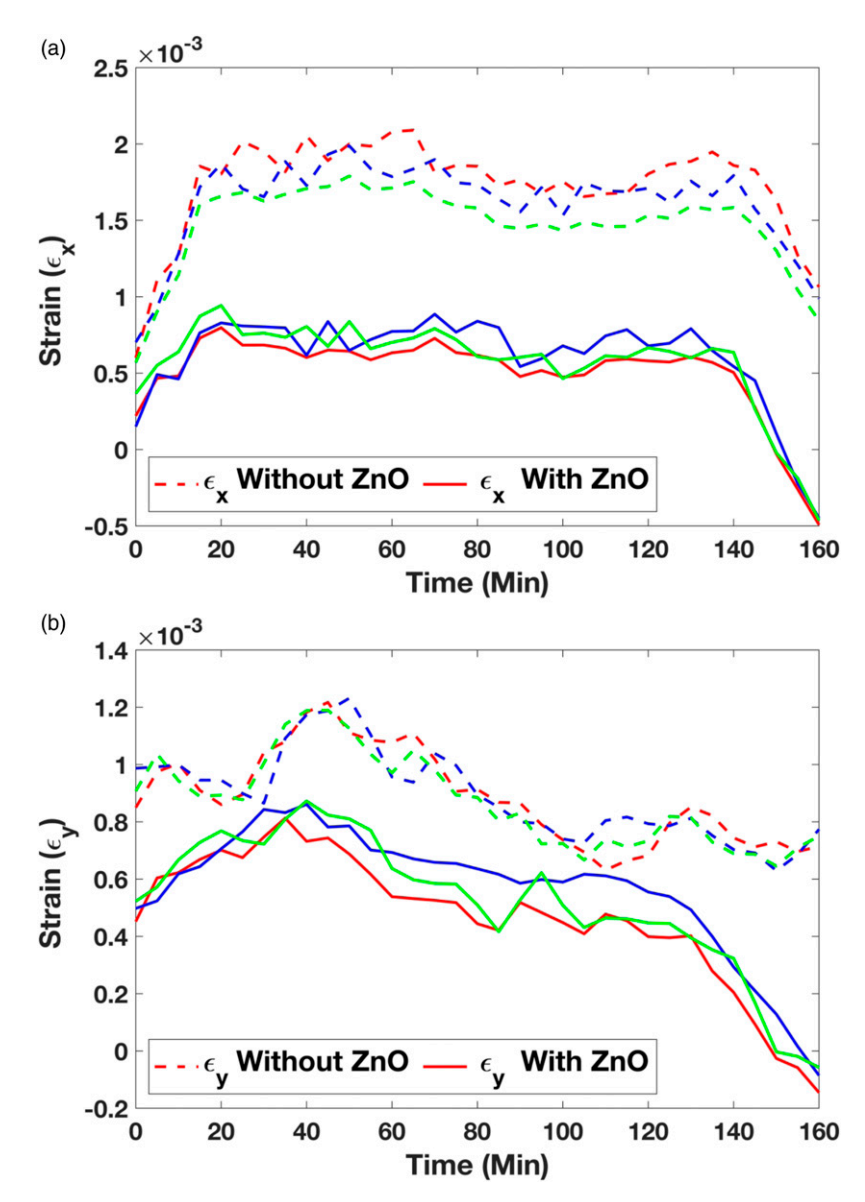


Figure 9. (a) In-Situ X-strain ( $\varepsilon_x$ ), and (b) Y-strain ( $\varepsilon_y$ ), for hybrid and reference laminates for  $[0^{\circ}/90^{\circ}]$  laminate.

residual stresses' evolution was observed for the ZnO modified composite laminate. For ZnO-enhanced composite laminates, a maximum residual stress of -29 MPa and -114 MPa was observed in x-direction and y-direction, respectively, as shown in Figure 12. For [0/90] composite laminates, the residual stress in the x-direction decreased by 30 MPa and in the y-direction by 111 MPa because of ZnO modification.

For  $[45^{\circ}/-45^{\circ}]$  composite laminates, residual stress remains nearly constant for the first 100 min of cure in both the x and y directions. From 100 to 150 min of curing, a maximum residual stress of 7.04 MPa and -10.82 MPa was observed for composites made with reference fibers in the x- and y-directions, respectively, as shown in Figure 13. Residual stress in ZnO enhanced composite laminates increases slowly

until 100 min and reaches 1.83 MPa in the x direction and -2.81 MPa in the y direction. From 100 to 130 min of curing, residual stress increases rapidly to a maximum of 4.12 MPa, then decreases to 2.09 MPa in the x direction between 130 and 150 min, as shown in Figure 14. While in the y direction, residual stress increased from 100 to 150 min and reached a maximum of -9.46 MPa, as shown in Figure 14. As a result of ZnO modification, the max residual stress in the x-direction decreased by 2.92 MPa and in the y-direction decreased by 1.36 MPa for [45/-45] composite laminates.

#### **Discussion**

Hybrid composites were fabricated by growing ZnO NWs on carbon fibers. Growth was achieved using a

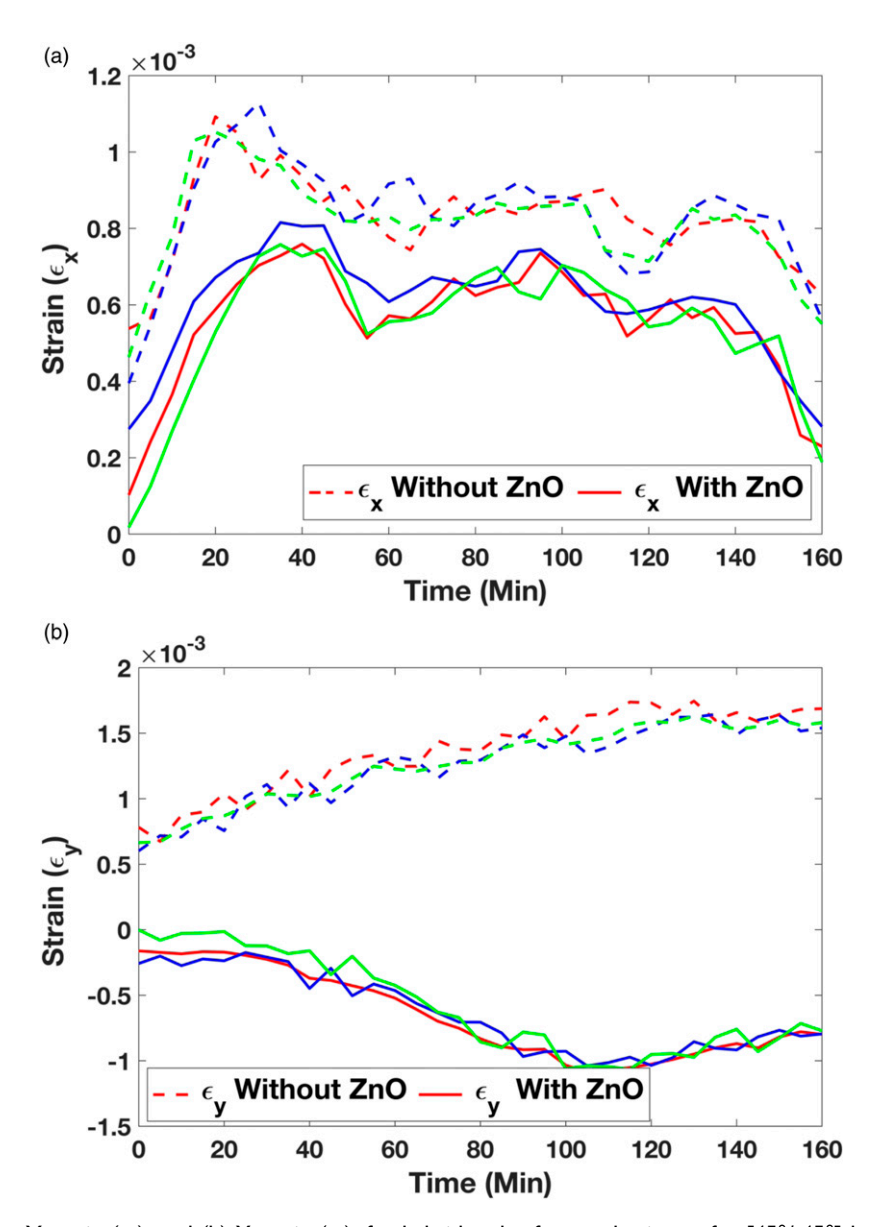


Figure 10. (a) In-Situ X-strain ( $\varepsilon_x$ ), and (b) Y-strain ( $\varepsilon_y$ ), for hybrid and reference laminates for [45°/-45°] laminate.

hydrothermal method. The hydrothermal process is a low-temperature technique for ZnO growth compared to others like CVD, therefore, did not cause severe fiber degradation. Various microstructural and thermomechanical characterization methods were utilized to analyze the effects of interface modification on the composite properties and the development of residual stresses. The ZnO NWs modification of the fibers improved both the axial and off-axis tensile properties and reduced the in situ strains and residual stresses during curing. The effect of the ZnO NWs is collectively guided by the following interrelated effects: (a) increase in fiber surface area, (b) stiffness increase, and (c) nanoscale tethering (i.e., mechanical interlocking).

The ZnO NWs significantly increase the surface area of the fibers. For example, a 50% coverage of a 7 μm diameter carbon fiber with 2 μm long, 800 nm diameter ZnO nanowires will result in a 500% increase in surface area of each fiber. The above dimensions are based on micrograph measurements. Additionally, ZnO NWs have higher thermal conductivity (60.0 W/m-K<sup>35</sup>) than carbon fiber (14 W/m-K<sup>36</sup>). The ZnO nanowires act as nanoscale fins and increase the heat transfer rate at the interface. This is captured in Figure 6, where fibers with ZnO modification cool at 2.07°C/min rate faster than reference fiber. During the curing, this increased surface area results in higher thermal gradients and degree of cure as shown in Figure 6 and Figure 7. The rapid cooling at the interface will reduce the

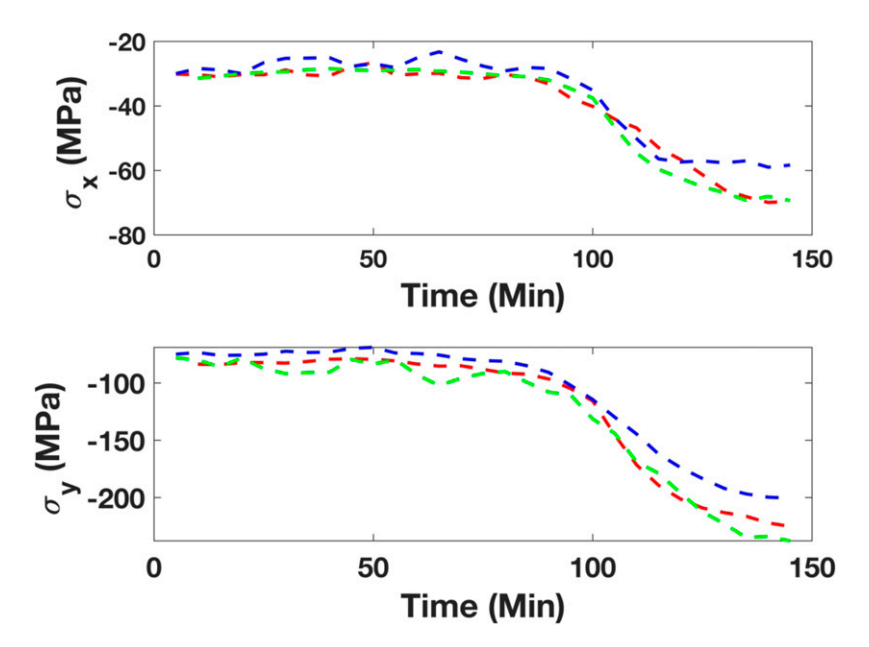


Figure 11. Residual stress evolution for [0°/90°] reference composite laminate.

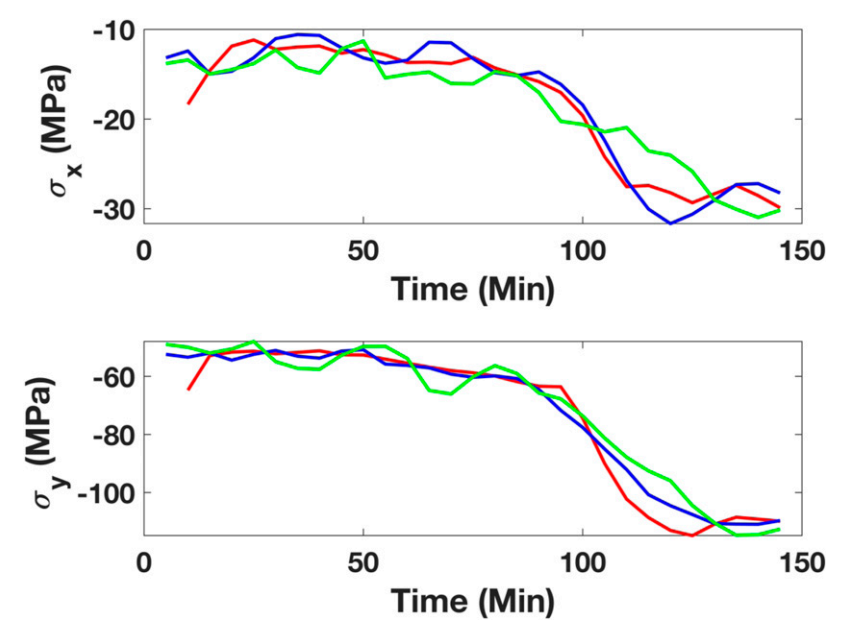


Figure 12. Residual stress evolution for ZnO modified composite for [0°/90°] laminate.

temperature of the surrounding matrix. Furthermore, at the interface region, the presence of ZnO NWs decreases the local thermal expansion of the interface region, which would also contribute to the lowering of residual stresses.

The addition of ZnO NWs is expected to increase the stiffness of each fiber. The ZnO NWs coating increases the original fiber diameter from 7  $\mu$ m to 10–11  $\mu$ m. Considering a 50% coverage of the fiber with ZnO NWs and the elevated ZnO elastic modulus of 800 GPa,<sup>37</sup> one can estimate the

increase in flexural stiffness (EIs) for an individual fiber. The estimated flexural stiffness of the individual fibers increased by approximately 396% due to ZnO NWs enhancement. The carbon fibers act collectively in woven bundles. The magnitude of stiffness increase would be lower than for an individual fiber, but nevertheless, an increase in stiffness is anticipated. This, in turn, results in reduced movement of plies during curing and can help reduce residual stresses.

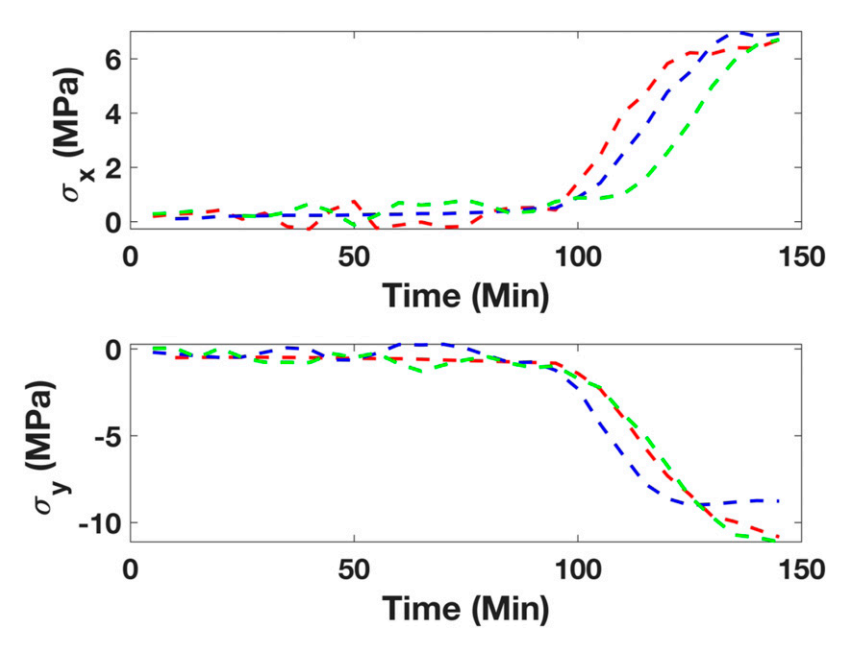


Figure 13. Residual stress evolution for [45°/-45°] reference composite laminate.

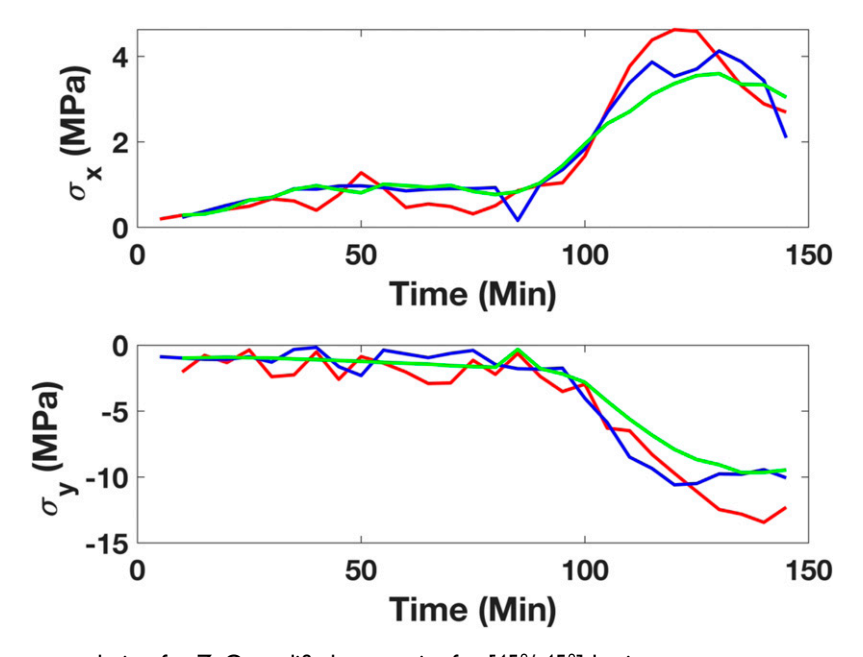


Figure 14. Residual stress evolution for ZnO modified composite for [45°/-45°] laminate.

Moreover, the ZnO NWs increase the friction between the plies and restrict the inter-ply movement of the laminate during curing by acting as mechanical tethers. This results in reducing the surface strain measured by DIC. As shown in Figures 9(a),(b) and Figure 10(a) composite laminate made by ZnO-modified fiber exhibits less strain in both directions than the reference composite for both layup configurations.

The addition of ZnO NWs has a significant effect on the elastic modulus and strength of the composites. In particular, the strength and stiffness increase significantly (by 130% and 280%, respectively) for the [45°/-45°] layup. Compared to [0°/90°], the mechanical behavior of [45°/-45°] configuration is governed by off-axis properties. The ZnO NWs enhancement may have improved the matrix performance at the interface because the off-axis properties are generally associated with matrix behavior.<sup>33</sup> The residual stresses are dependent on the layup. We explored this aspect using the in situ analysis

approach in an earlier study.<sup>24</sup> In particular, unbalanced residual stresses in asymmetric layups can cause warpage due to extension-bending and shear couplings. This is usually not desirable but is sometimes useful, e.g., bistable laminates.<sup>38</sup> While we focused on symmetric layups in this work, the ability of ZnO NWs enhancement to reduce residual stresses can potentially be used to reduce warpage in asymmetric layups.

Several studies use matrix modification to reduce residual stresses by improving matrix properties.<sup>21</sup> Here, we modified the fibers instead, thereby concentrating the nanophase's effect at the interface region. This results in engineering the critical interface region, which influences many behaviors, including residual stresses.

#### **Conclusion**

The primary conclusions of the study are as follows:

- (a) Micrographs showed that the hydrothermal chemical synthesis led to a uniform coverage of radially grown ZnO nanowires with similar lengths and diameters.
- (b) Thermal analysis showed that the ZnO NWs enhanced the cooling rate during the curing by 2.07°C/min, resulting in a higher degree of cure at the interface region.
- (c) The ZnO NWs modification contributed to an enhancement in strength and apparent elastic modulus. For the [0°/90°] and [45°/-45°] laminates, the strength increased by 20% and 130%, respectively. Whereas the apparent elastic modulus for the [0°/90°] composite laminate improved by 9% and for the [45°/-45°] laminate by 280%.
- (d) Digital image correlation was used to analyze the evolution of strain in the composites during autoclave processing. ZnO interface modification resulted in the reduction of in situ strains during curing. The maximum values of the strains in X and Y directions ( $\varepsilon_x$  and  $\varepsilon_y$ ) were reduced by 55% and 31%, respectively, for the [0°/90°] laminate. For the [45°/-45°] laminate, the maximum  $\varepsilon_x$  and  $\varepsilon_y$  were reduced by 27.31% and 166.26%, respectively.
- (e) Residual stresses were evaluated using in situ strains and temperature-dependent elastic properties. The hybrid composites also exhibited lower residual stresses during curing. The residual stresses in the *X* and *Y* directions were reduced by 50.8% and 49.3%, respectively, for the [0°/90°] composite laminate. The residual stresses for the [45°/-45°] composite laminate were reduced by 41.47% and 17.8% in the *X* and *Y* directions, respectively.

In conclusion, the growth of ZnO NWs using hydrothermal chemical growth is an effective method for improving mechanical properties and reducing residual stresses in carbon fiber epoxy composites.

#### **Acknowledgements**

We thank Dr. Sandra Boetcher and Dr. Jeff Brown for their support in using the DSC machine and thermal imaging camera, respectively.

#### **Declaration of conflicting interests**

The author(s) declared no potential conflicts of interest with respect to the research, authorship, and/or publication of this article.

#### **Funding**

The author(s) disclosed receipt of the following financial support for the research, authorship, and/or publication of this article: This research was supported by National Science Foundation (NSF) Advanced Manufacturing Grant (2001038).

#### **ORCID iD**

Sirish Namilae https://orcid.org/0000-0003-1487-9573

#### References

- Das S. Life cycle assessment of carbon fiber-reinforced polymer composites. *Int J Life Cycle Assess* 2011; 16: 268–282. doi: 10.1007/s11367-011-0264-z
- Soutis C. Fibre reinforced composites in aircraft construction. Progress in Aerospace Sciences 2005; 41: 143–151. doi: 10. 1016/j.paerosci.2005.02.004
- Vedrtnam A and Sharma SP. Study on the performance of different nano-species used for surface modification of carbon fiber for interface strengthening. *Composites Part A: Appl Sci Manufact* 2019; 125: 105509. doi: 10.1016/j.compositesa. 2019.105509
- Boroujeni AY, Tehrani M, Nelson AJ, et al. Hybrid carbon nanotube-carbon fiber composites with improved in-plane mechanical properties. *Compos B Eng* 2014; 66: 475–483. doi: 10.1016/j.compositesb.2014.06.010
- Ouyang H, Zhou M, Fei J, et al. Grafting the buffer interphase "MOF-5" for acquiring carbon fiber reinforced composite with excellent mechanical and tribological properties. *J Appl Polym Sci* 2022; 139: 51493. doi: 10.1002/app.51493
- Yang J, Xiong J, Ma L, et al. Vibration and damping characteristics of hybrid carbon fiber composite pyramidal truss sandwich panels with viscoelastic layers. *Compos Struct* 2013; 106: 570–580. doi: 10.1016/j.compstruct. 2013.07.015
- 7. Liu H, Huang G, Wang R, et al. Carbon nanotubes grown on the carbon fibers to enhance the photothermal conversion toward solar-driven applications. *ACS Appl Mater*

- Interfaces 2022; 14: 32404–32411. doi: 10.1021/acsami. 2c07970
- Malakooti MH and Sodano HA. Multi-Inclusion modeling of multiphase piezoelectric composites. *Compos B Eng* 2013; 47: 181–189. doi: 10.1016/j.compositesb.2012.10.034
- Poges S, Monteleone C, Petroski K, et al. Preparation and characterization of an oxide-oxide continuous fiber reinforced ceramic matrix composite with a zinc oxide interphase. *Ceram Int* 2017; 43: 17121–17127. doi: 10.1016/j.ceramint. 2017.09.133
- Masghouni N and Al-Haik M. Computational molecular dynamics study of hybrid composite incorporating ZnO nanowires. *J Comput Theor Nanosci* 2015; 12: 665–673. doi: 10.1166/jctn.2015.3784
- Marashizadeh P, Abshirini M, Wang J, et al. Multiscale modeling of fiber fragmentation process in aligned ZnO nanowires enhanced single fiber composites. *Sci Rep* 2019; 9: 19964. doi: 10.1038/s41598-019-56503-x
- 12. Marashizadeh P, Abshirini M, Saha M, et al. Numerical interlaminar shear damage analysis of fiber reinforced composites improved by zno nanowires. In: ASME International mechanical engineering Congress and Exposition, Proceedings (IMECE), Virtual, Online, November 16–19, 2020. New York, NY: ASME, 2020. doi: 10.1115/IMECE2020-23422
- Lutz T, Yue X and Camelio J. Towards a digital twin: Simulation and residual stress analysis in aerospace composite structures assembly. In: Proceedings of ASME 2022 17th International manufacturing Science and engineering Conference, West Lafayette, IN, USA, June 27–July 1, 2022. West Lafayette, IN: ASME, 2022. doi: 10.1115/MSEC2022-85439
- 14. Shokrieh MM and Ghanei Mohammadi AR. The importance of measuring residual stresses in composite materials. *Residual stresses in Composite Materials* 2021; 2014: 3–14. doi: 10.1016/B978-0-12-818817-0.00017-2
- Maxwell AS, Broughton WR and Lodeiro MJ. Review of techniques for the characterisation of residual stress in polymer composites. NPL report. Middlesex, UK: National Physocal Laboratory. Available at: http://eprintspublications. npl.co.uk/id/eprint/3757
- Huang ZM. Strength formulae of unidirectional composites including thermal residual stresses. *Mater Lett* 2000; 43: 36–42. doi: 10.1016/S0167-577X(99)00227-X
- 17. Zhou W, Zhou H, Zhang R, et al. Measuring residual stress and its influence on properties of porous ZrO2/(ZrO2+Ni) ceramics. *Materials Science and Engineering A* 2015; 622: 82–90. doi: 10.1016/j.msea.2014.11.018
- Parlevliet PP, Bersee HEN and Beukers A. Residual stresses in thermoplastic composites-A study of the literature-Part I: Formation of residual stresses. *Composites Part A: Applied Science and Manufacturing* 2006; 37: 1847–1857. doi: 10. 1016/j.compositesa.2005.12.025

- Nairn JA. Matrix microcracking in composites. *Polymer Matrix Composites* 2000; 2: 403–432.
- 20. Quek MY. Analysis of residual stresses in a single fibre-matrix composite. *Int J Adhes Adhes* 2004; 24: 379–388. doi: 10.1016/S0143-7496(03)00097-6
- Shokrieh MM and Safarabadi M. Effects of imperfect adhesion on thermal micro-residual stresses in polymer matrix composites. *Int J Adhes Adhes* 2011; 31: 490–497. doi: 10. 1016/j.ijadhadh.2011.04.002
- Nishino T, Kotera M and Sugiura Y. Residual stress of particulate polymer composites with reduced thermal expansion. *Journal Phys: Conf Ser* 2009; 184: 012026. doi: 10. 1088/1742-6596/184/1/012026
- 23. Chava S and Namilae S. In situ investigation of the kinematics of ply interfaces during composite manufacturing. *J Manuf Sci Eng* 2021; 143(2): 021006.
- Chava S and Namilae S. Continuous evolution of processing induced residual stresses in composites: An in-situ approach. Compos Part A Appl Sci Manuf 2021; 145: 106368. doi: 10. 1016/j.compositesa.2021.106368
- Chava S, Namilae S and Al-Haik M. Residual stress reduction during composite manufacturing through cure modification: In situ analysis. *J Compos Mater* 2022; 56: 975–988. doi: 10. 1177/00219983211066545
- 26. Ayyagari S, Al-Haik M and Rollin V. Mechanical and electrical characterization of carbon fiber/bucky paper/zinc Oxide hybrid composites, *C (Basel)* 2018; 4(1): 6. doi: 10. 3390/c4010006
- ASTM International. Standard test method for tensile properties of polymer matrix composite materials D3039.
  West Conshohocken, PA, USA: American society for testing and Materials, 2014.
- 28. ASTM International. D7028-07 standard test method for glass transition temperature (DMA tg) of polymer matrix composites by dynamic mechanical analysis (DMA). West Conshohocken, PA, USA: American society for testing and Materials, 2007.
- 29. Roşu D, Caşcaval CN, Mustată F, et al. Cure kinetics of epoxy resins studied by non-isothermal DSC data. *Thermochim Acta* 2002; 383: 119–127. doi: 10.1016/S0040-6031(01)00672-4
- Cruz-Cruz I, Ramírez-Herrera CA, Martínez-Romero O, et al. Influence of epoxy resin curing kinetics on the mechanical properties of carbon fiber composites, *Polymers (Basel)* 2022; 14(6): 1100. doi: 10.3390/polym14061100
- Johnson RR, Kural MH and Mackey GB. Thermal expansion properties of composite materials. California, USA: Sage Publications 1981.
- 32. Tehrani M, Boroujeni AY, Hajj R, et al. Mechanical characterization of a hybrid carbon nanotube/carbon fiber reinforced composite. In: ASME International mechanical engineering Congress and Exposition, Proceedings (IMECE), San Diego, CA, USA, November 15–21, 2013. California, USA: ASME, 2013. doi: 10.1115/IMECE2013-62251

33. Kaw AK. *Mechanics of composite materials 2nd*, USA: Optica 2006.

- 34. Nairn JA and Zoller P. Matrix solidification and the resulting residual thermal stresses in composites. *J Mater Sci* 1985; 20: 355–367. doi: 10.1007/BF00555929
- 35. Williams ML. CRC handbook of chemistry and physics 76th edition, *Occup Environ Med* 1996; 53: 504. doi: 10.1136/oem.53.7.504
- 36. Cytec engineered materials. *Technial data sheet. Thornel T650/35 PAN-Based Fiber*. USA: Cytec Engineered
- Materials, 2012. https://www.fibermaxcomposites.com/shop/datasheets/T650.pdf
- Soomro MY, Hussain I, Bano N, et al. Nanoscale elastic modulus of single horizontal ZnO nanorod using nanoindentation experiment. *Nanoscale Res Lett* 2012; 7: 146. doi: 10.1186/1556-276X-7-146
- Mukherjee A, Ali SF and Arockiarajan A. Hybrid bistable composite laminates for structural assemblies: Numerical and experimental study. *Compos Struct* 2021; 260: 113467. doi: 10.1016/j.compstruct.2020.113467